

Validation of the Modeling of a Commercial Extrapolation Chamber using the Monte Carlo
Technique

Priscilla R. T. L. Camargo, Hélio Yoriyaz, Paulo T. D. Siqueira, and Linda V. E. Caldas*

Instituto de Pesquisas Energéticas e Nucleares (IPEN-CNEN)

Comissão Nacional de Energia Nuclear

Av. Prof. Lineu Prestes, 2242, 05508-000, São Paulo, SP, Brazil

Tel/Fax: +55 11 3133 9716

E-mail: priscilla@usp.br

E-mail: hyoriyaz@ipen.br

E-mail: ptsiquei@ipen.br

E-mail: lcaldas@ipen.br

5 Abstract: In order to determine the correction factors that have to be taken into account for accurate measurements of air kerma rates for low energy X-rays utilizing extrapolation chambers, a PTW extrapolation chamber (model 23391) was modeled using the MCNP code. To validate this modeling, two tests were performed: determination of energy dependence and extrapolation curves. The results obtained from simulations are in good agreement with the measured results. The main contribution of the specific correction factors for the extrapolation chamber were determined.

*corresponding author

Keywords: extrapolation chamber, low energy X-rays, Monte Carlo simulations, corrections factors.

INTRODUCTION

Extrapolation chambers are basically a parallel plate ionization chamber, that allow variation of the air mass inside them due to changes in their sensitive volume through the variation of the inter-electrode distance (Zankowski and Podgorsak, 1997). These chambers are commonly utilized for determination of superficial doses, since it is possible to determine the air kerma rate for a null distance between the electrodes, by extrapolating the experimental curve of accumulated charge versus the distance between the electrodes.

The first model of extrapolation chamber was developed by Failla in 1937 (Failla, 1937). At that time the potential use of these chambers for superficial dose determination had already been verified. Böhm and Schneider (Böhm and Schneider, 1986) studied deeply the response of these detectors for soft radiations. Furthermore, the extrapolation chambers are frequently utilized in phantom arrangements mainly for the determination of absolute doses in water due soft radiations (Böhm, 1979; Soares et al, 1998; DeBlois et al, 2002).

Therefore, extrapolation chambers have become very important metrological instruments for detection of soft radiations. Besides accurately determining the air kerma rate for low energy X-rays and beta radiation, extrapolation chambers present dimensional advantages in relation to other chambers. Thus, they have shown their utility as primary standard for soft radiations (Soares, 2001; Dias and Caldas, 2001; Oliveira and Caldas, 2005).

In order to establish a primary standard for radiations it is necessary to completely characterize the ionization chamber, by determining the correction factors related with physical aspects of the detector, and to maintain proper laboratory conditions. For beta radiation the extrapolation chambers are used in the main international metrological laboratories as primary standards for accurate measurements of absorbed doses (Soares, 1991; Helmstädter et al, 2004; Behrens et al, 2007).

For low and medium energy X-rays, the free-air chamber are usually utilized as primary standard in metrology laboratories for the determination of air kerma rates (Burns et al, 2003; Burns, 2004; Cullberson et al, 2006). However, extrapolation chambers are useful detectors for accurate measurements for soft X-rays beams too. Some authors have investigated the establishment of extrapolation chambers as primary standards for low energy X-rays or as main instruments for the determination of absorbed doses in X-rays beam qualities (Böhm and Schneider, 1986; Kotler, 2002).

In recent years, some correction factors for primary standards for low energy radiation have been determined by Monte Carlo simulations, since the obtained results are most of time more accurate than the experimental values. Moreover, it is possible, through this technique to get a better comprehension about the physical aspects of each factor involved in the measurements (Burns, 2003; Selvam et al, 2005; Abdel-Rahman et al, 2005; Burns, 2006).

In the present work, a commercial extrapolation chamber PTW model (23391) was modeled using the MCNP code. This model was validated comparing the extrapolation curve and the energy dependence behavior of the chamber determined experimentally and by Monte Carlo simulations. The specific correction factors were established for this chamber in soft X-rays

diagnostic radiology level. The potential use of the extrapolation chambers as a primary standard for measurements of low energy X-rays was carefully discussed, and the most significant correction factors were quantified.

MATERIALS AND METHODS

A commercial extrapolation chamber PTW model (23391) was utilized in this work. The chamber inter-electrode distance can be varied from 0.5 mm to 25.0 mm using a micrometric device. The collecting electrode (diameter: 40.0 mm) and the guard ring are made of Aluminum; the entrance window is made of a 0.025 mm thick polyamide foil

A Pantak/Seifert X-rays system, with tube operating from 5 kV to 160 kV was utilized, the detector was positioned at 1.00 m of distance from the X-rays focal spot. An electrometer Keithley 617 was connected to the extrapolation chamber for the charge measurements.

For the determination of the extrapolation curve the standard beam conditions RQR3 (50 kV, 100 mA) were maintained constant, and the inter-electrode distance of the chamber was varied from 0.7 mm to 3.0 mm.

For the test of energy dependence, the distance between the electrodes was fixed at 1.5 mm, and ionization current measurements were taken for several beam qualities (diagnostic radiology level) in accordance with the recommendations of the IEC 61674 (IEC 61674, 1997). Table 1 shows the specifications of the diagnostic radiology level beams qualities established in the Instruments Calibration Laboratory (LCI) of Nuclear and Energy Research Institute (IPEN) – São Paulo - Brazil.

The calibration coefficients were determined by the substitution technique, where it was utilized a parallel plate ionizing chamber PTW 77334 as reference secondary standard.

SIMULATIONS

In order to better understand the main contributions to the collected charge of the extrapolation chamber in the performed experiments, sets of simulations were run using the MCNP-5 code. MCNP (Briesmeister, 2000) is a Monte Carlo based radiation transport code that can transport electrons and photons with energies ranging from 1 keV up to many MeV. Besides being a very confident and benchmarked code, one of its main potentialities rests in its capability to geometrically describe very well detailed systems.

Simulations were performed into two parts:

- X-Ray Spectra: mono energetic electron beams were modeled impinging on the Tungsten anode. The produced photon spectra were then recorded after a 2.5 mm Al filtration. A specific simulation was performed for each beam quality to properly characterize the photon field in which the extrapolation chamber was inserted; and
- Extrapolation Chamber: the PTW extrapolation chamber was modeled. All of its main structures were represented. A photon radiation field was made to impinge on extrapolation chamber front wall, and the energy deposited in its collecting volume was tallied.

This approach, which consists of the obtainment of the source specification (X-ray spectra) and the desired tally (energy deposition in the collecting volume), was adopted aiming to speed up simulations, as many simulations were performed for the same radiation field. The geometric description of each part can be seen in Figures 1 and 2.

RESULTS AND DISCUSSION

Extrapolation curve

For the experimental determination of the extrapolation curve, measurements of the accumulated charge versus the inter-electrode distance were made. The measurements uncertainties showed values lower than 0.07%. The extrapolation chamber presented a linear behavior from 0.5 mm to 2.0 mm. Figure 3 shows the complete experimental extrapolation curve while Figure 4 shows only its linear response range.

Energy dependence

For the experimental test of energy dependence, measurements of ionization accumulated charge for several beam qualities were carried on. Figure 5 shows the results of simulations for accumulated charge per incident electrons energy. Calibration coefficients were determined by the substitution technique, utilizing a secondary standard for soft X-rays, a parallel plate chamber PTW 77334. Table 2 shows the extrapolation chamber calibration coefficients (F_c), obtained for beam radiation qualities (diagnostic radiology level) evaluated, the results shows a maximum variation of 5.6%. Table 2 also presents the calibration coefficients determined by Monte Carlo simulations, the comparison between the measured and simulated calibration coefficients will be discussed further.

SIMULATIONS

Extrapolation Curve

A simulated extrapolation curve was obtained for the RQR3 quality beam by varying the distance between the structures that represent the back electrode. All moving structures were moved to reproduce the real geometry of the extrapolation chamber. The simulated extrapolation curve is shown in Figure 6. Results are presented in terms of the energy imparted to the collecting volume per source photon. As MCNP-5 does not consider the electric field between the electrodes, electrons do move through the surfaces that involves the collecting volume.

To get a glance of the effects of this movement through the surfaces that embrace the collecting volume, a set o simulations was carried out with electrons movements turned off. Results showed substantial decrease in the amount energy imparted to the collecting volume without qualitatively changing the behavior of the extrapolation curve shown. The amount of charge flowing through the embracing surfaces was an extra tally added to the simulations as an intent to broad the comprehension of the simulation results.

Figure 7 shows the experimental and the simulated results for complete extrapolation curve. The amount of charge escaping from the collecting volume is also plotted. As the inter-electrode distance increases the experimental results depart from the linear behavior as was mentioned earlier. Charge flow from the collecting volume presents a similar trend: a linear response to the inter-electrode distance increase for the bottom range of the extrapolation curve; and a departure

from this trend above 3.0 mm. Charge flow however seems to reach a top value as the characteristics length of the experiments exceeds electrons mean free path.

Energy Dependence

For a specific disposition of the extrapolation chamber (1.5 mm inter electrode distance), different beam qualities/energies were made to impinge the on the extrapolation chamber front wall. The energy dependence simulated results are shown in Figure 8. Here again, results are presented in terms of the energy imparted to the collecting volume per source photon, therefore, effects of beam intensity related to each field quality have not been considered. Charge flowing from the collecting volume is also shown.

Utilizing the obtained values of collected charge for each quality beams in the same conditions of the experiments, it was determined the simulated calibration coefficients by means the substitution technique. For this the parallel plate PTW 77334 chamber was also utilized as reference.

The table 2 presents either the calibrations coefficients measured and simulated. The simulated values presented maximum variation of 5.8%. In accordance with the results showed in table 2 and in figure 6 it is possible to conclude that test of energy dependence simulated presented a good behavior and it is in agreement with the experimental results.

Correction Factors

Side contributions to the delivered energy in the collecting volume, i.e., contributions that do not come directly from the incident beam were also evaluated for the main contributors. The main side contributions to the delivered energy to the collecting volume, i.e. the amount of tallied energy which do not come straight from the filter through the extrapolation window, can be distinguished by their path:

- Through the front wall;
- Scattered at the side encasement;
- Backscattered from the moving electrode..

Their relative contribution were tallied in different simulations ran just after a record file of particles crossing these structures was created in a regular run. These record files were used as tagged source particles in which only the particles attaining a set of characteristic (populating a specific part of the phase space) were simulated and transported by MCNP in a specific run. As these contributions change due to geometric change of electrode displacement as well as due to the field quality, just few experimental arrangements have been considered. Table 3 shows these relative contributions.

CONCLUSIONS

Monte Carlo modeling of the commercial extrapolation chamber PTW 23391 was validated. The measured and simulated results of the two tests: extrapolation curve and energy dependence were in agreement. Therefore, this model could be utilized to determine the main correction factors for the extrapolation chamber.

The correction factors depend heavily on the geometry of the detector, and on the position of the equipment in relation to the radiation beam. In this work, it was possible to specify the main side contribution of the extrapolation chamber in the case in that it was irradiated with low energy X-rays in diagnostic radiology level. Table 3 shows that the collecting electrode backscattering stands as the main side contribution source (30% of the doses values).

Results show that this set-up is not an adequate one to use the extrapolation chamber as a primary standard for low energy X-rays diagnostic radiology level. However, in a set-up with the chamber in a phantom the backscattering in the collecting electrode probably will decrease substantially, and the extrapolation chamber could be utilized as a primary standard for these irradiation conditions. In radiotherapy levels, where the extrapolation chamber is closer to the X-rays focal spot, the backscattering will probably have lower contribution to the doses values.

Simulations provide a a substantial set of information which enables to better understand the role played by different components related to of each individual correction factor.

For measurements of low energy X-rays with extrapolation curve, there are no works in literature that investigate deeply the physical aspects of these quantities. This work, present some questions and answer to better set-up an experiment for a proper use of the extrapolation chamber as a primary standard for these range of x-Rays energies.

ACKNOWLEDGMENTS

The authors are thankful to Conselho Nacional de Desenvolvimento Científico e Tecnológico (CNPq) and to Fundação de Amparo à Pesquisa do Estado de São Paulo (FAPESP), Brazil, for partial financial support of this work.

REFERENCES

- Abdel-Rahman, W., Seuntjens, J. P., Verhaegen, F., Deblois, F., Podgorsak, E. B., 2005. Validation of Monte Carlo surface doses for megavoltage photon beams. *Med. Phys.*, 32, 286-298.
- Behrens, R., Helmstädter, K., Ambrosi, P., Bordy, J-M., Lecante, C., Bovi, M. I Jokelainen, I., Soares, C. G., Saull, P. R. B., Kharitonov, I. A., Fedina, F., Kurosawa, T., Kato, M., 2007. International comparison EUROMET.RI(I)-S2 of extrapolation chamber measurements of the absorbed dose rate in tissue for beta radiation (EUROMET project No 739): Final report. *Metrol.*, 44.
- Böhm, J., 1979. The perturbation correction factor of ionization chambers in β -radiation fields. *Phys. Med. Biol.*, 25, 65-75.
- Böhm, J., Schneider, U., 1986. Review of extrapolation chamber measurements of beta rays and low energy X-rays. *Radiat. Protec. Dosim.*, 14, 193-198.
- Briesmeister J.F., 2000. MCNP: A general Monte Carlo N-particle transport code, version 4C. LA-13709-M, Los Alamos Scientific Laboratory, Los Alamos, New Mexico
- Burns, D. T., O' Brien, M., Lamperti, P., Boutillon, M., 2003. Comparison of the NIST and BIPM medium-energy X-ray air-kerma measurements. *J. Resear. Nat. Inst. Stand. Techn.*, 108, 383-389.
- Burns, D. T., 2003. Degrees of equivalence for the key comparison BIPM.RI(I)-K3 between national primary standards for medium-energy x-rays. Report BIPM.RI(I).K3.

Burns, D.T., 2006. A new approach to the determination of air kerma using primary-standard cavity ionization chambers. *Phys. Med. Biol.*, 51, 929-942.

Burns, D., 2004. Changes to the BIPM primary air-kerma standards for X-rays. *Metrol.*, 41, L3.

Culberson, W. S., DeWerd, L. A., Anderson, D. R., Micka, J. A., 2006. Large-volume ionization chamber with variable apertures for air-kerma measurements of low-energy radiation sources. *Rev. Scient. Inst.*, 77.

DeBlois, F., Abdel-Rahman, W., Seuntjens, J. P., Podgorsak, E. B., 2002. Measurement of absorbed dose with a bone-equivalent extrapolation chamber. *Med. Phys.*, 29, 433-440.

Dias, S. K., Caldas, L.V.E., 2001. Extrapolation chamber response in low-energy X radiation standard beams. *J. Appl. Phys.*, 89, 669-671.

Failla, G., 1937. Measurement of tissue dose in terms of the same unit for all ionizing radiations. *Radiol.*, 29, 202-215.

Helmstädter, K., Böhm, J., Ambrosi, P., Fominych, V., Rumyantseva, E., Fedina, S., 2004. Comparison of extrapolation chamber measurements of the absorbed dose rate for beta radiation between VNIIM (Russia) and PTB (Germany). *Metrol.*, 41.

International Electrotechnical Commission, 1997. Medical electrical equipment - Dosimeters with ionization chambers and/or semi-conductor detectors as used in X-ray diagnostic imaging. (IEC 61674).

Kotler, L., 2002. Absorbed dose calibrations at X-ray qualities, a viable alternative? Austral.Phys. Eng. Scien. Med., 25, 182.

Oliveira, M. L., Caldas, L. V. E., 2005. A special mini-extrapolation chamber for calibration of $^{90}\text{Sr}+^{90}\text{Y}$ Sources. Phys. Med. Biol., 50, 2929-2936.

Selvam, T. P., Saull, P. R. B., Rogers, D. W. O., 2005. Monte Carlo modeling of the response of NRC's $^{90}\text{Sr}/^{90}\text{Y}$ primary beta standard. Med. Phys., 32.

Soares, C. G., 1991. Calibration of ophtalmic applicators at NIST: A revised approach. Med. Phys., 18, 787-793.

Soares, C. G., Halpern, D. G., Wang, C.-K., 1998. Calibration and characterization of beta-particle sources for intravascular brachytherapy. Med. Phys., 25, 339-346.

Zankowski, C. E., Podgorsak, E. B., 1997. Calibration of photon and electron beams with an extrapolation chamber. Med. Phys., 24, 497.

Table1 – Qualities beams specifications establishes in the instruments calibration laboratory (LCI) in accordance with the recommendations of IEC 61674

Beam Qualities	Voltage (kV)	1° HVL (mmAl)	Effective Energy (keV)
RQR3	50	1.79	27.15
RQR4	60	2.09	28.80
RQR5	70	2.35	30.15
RQR6	80	2.65	31.65
RQR7	90	2.95	33.05
RQR8	100	3.24	34.40
RQR9	120	3.84	37.05

Table 2 – Energy dependence of the extrapolation chamber PTW 23391 (measured and simulated values)

Beam Qualities	Voltage (kV)	Calibration Coefficient (FC) normalized to RQR5 (Measured)	Calibration Coefficient Uncertainty (FC)% (Measured)	Calibration Coefficient (FC) normalized to RQR5 (Simulated)	Calibration Coefficient Uncertainty (FC)% (Simulated)
RQR3	50	1.001	0.240	0.946	0.761
RQR5	70	1.000	0.148	1.000	1.332
RQR7	90	1.019	0.113	0.985	1.071
RQR8	100	1.031	0.112	0.970	0.981
RQR9	120	1.056	0.103	1.007	0.702

Table 3- Relative contributions to the amount of energy deposited in the collecting volume of the extrapolation. Simulated results for RQR3 beam quality and distinct inter-electrode distances.

Inter-electrode distance (mm)	Backscattered from moving electrode (%)	Trespassing the front wall (%)	Total Side contributions (%)
0.5	42.3 (20)	14.6 (10)	56.9 (24)
0.75	38.2 (16)	11.9 (9)	50.1 (20)
1.0	34.7 (15)	9.4 (7)	44.0 (17)
1.5	31.4 (12)	8.8 (6)	40.1 (14)
3.0	27.0 (11)	7.4 (5)	34.4 (12)
5.0	22.3 (8)	4.5 (3)	26.8 (9)
6.0	20.6 (7)	3.87 (25)	24.5 (7)
8.5	16.6 (5)	2.86 (19)	19.4 (6)
11.0	14.1 (4)	2.05 (14)	16.1 (4)
16.0	11.4 (3)	1.26 (9)	12.7 (3)
21.0	9.6 (3)	1.04 (7)	10.6 (3)

Figure captions:

Figure 1 – Extrapolation Chamber simulated description.

Figure 2 – Schematic representation of the X-ray tube.

Figure 3 – Complete experimental extrapolation chamber curve.

Figure 4 – Linear part of the experimental extrapolation chamber.

Figure 5 – Experimental energy dependence curve

Figure 6 – Simulated and measured extrapolation curve (linear part).

Figure 7 – Simulated and measured complete extrapolation curve.

Figure 8 – Simulated energy dependence curve.

Figure 9 – Side contributions to energy imparted to the collecting volumes for a distinct inter-electrode spacings.

Figure 10 – Relative contribution to energy imparted to the collecting volumes by side contributions for a distinct inter-electrode spacings.

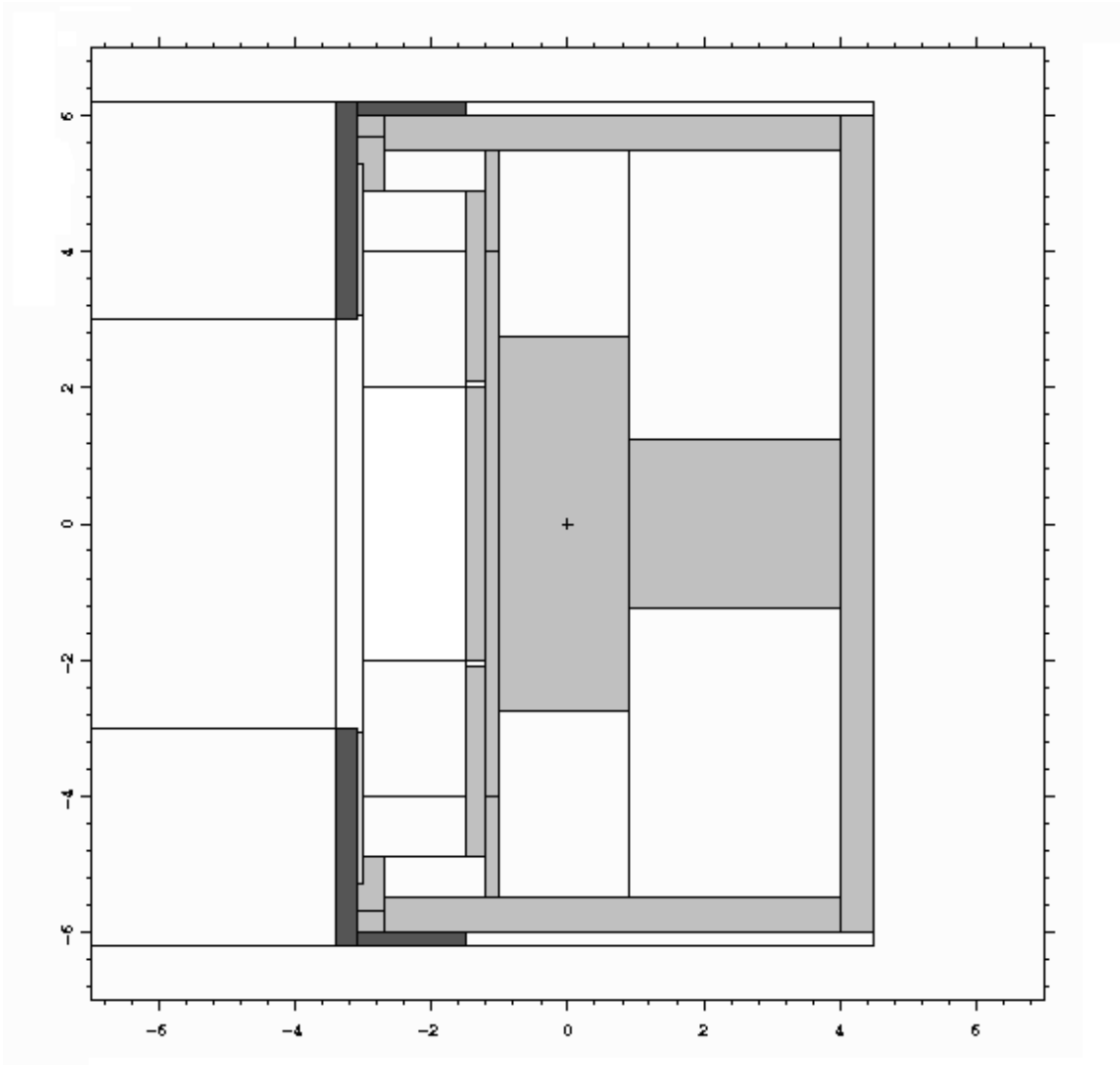


Figure 1

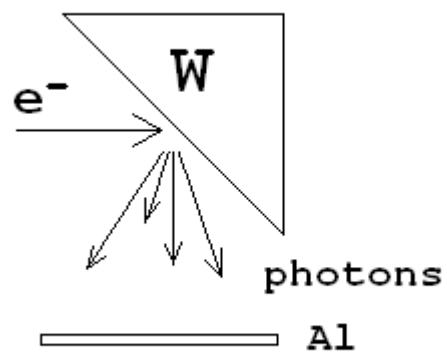


Figure 2

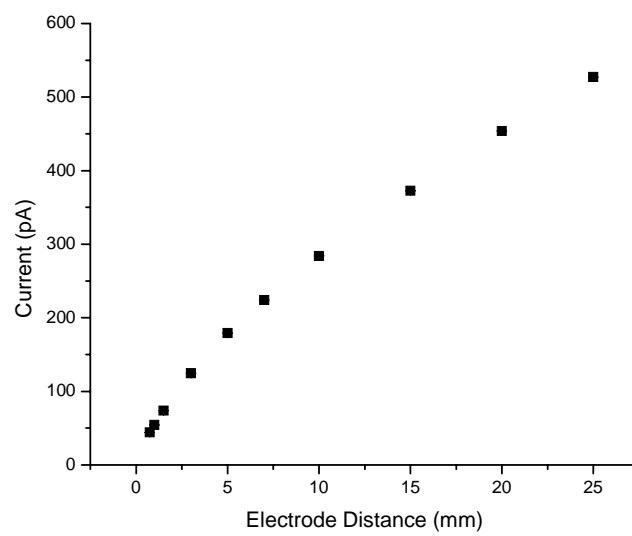


Figure 3

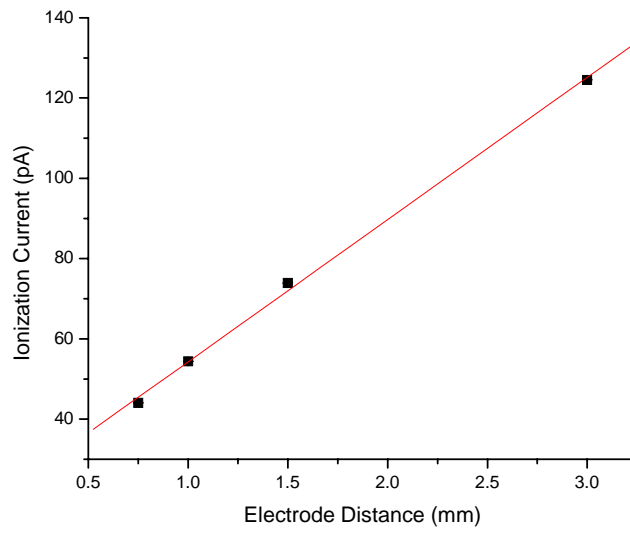


Figure 4

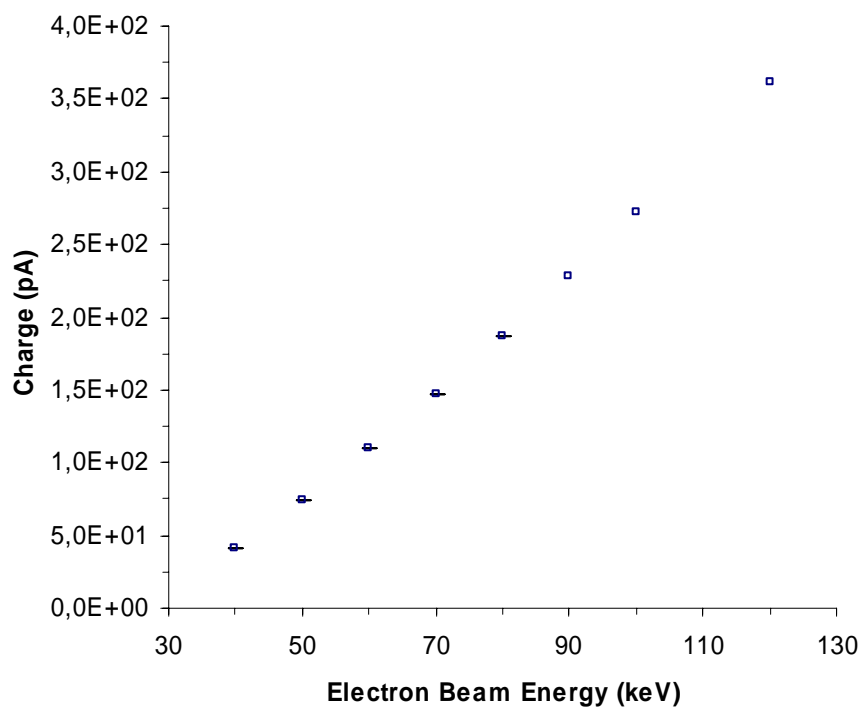


Figure 5

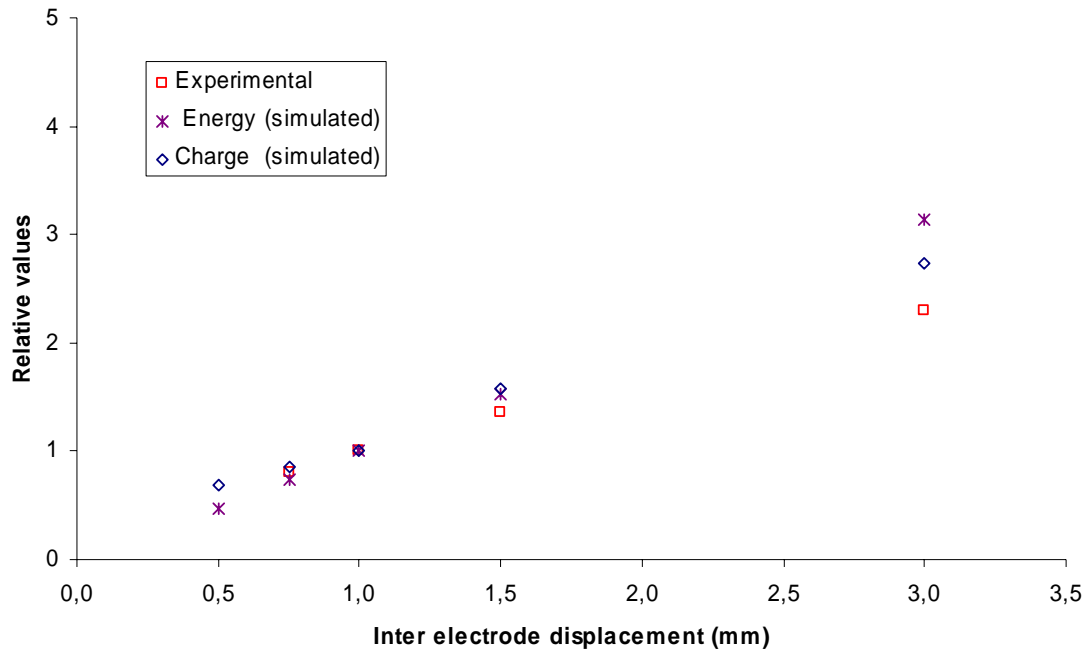


Figure 6

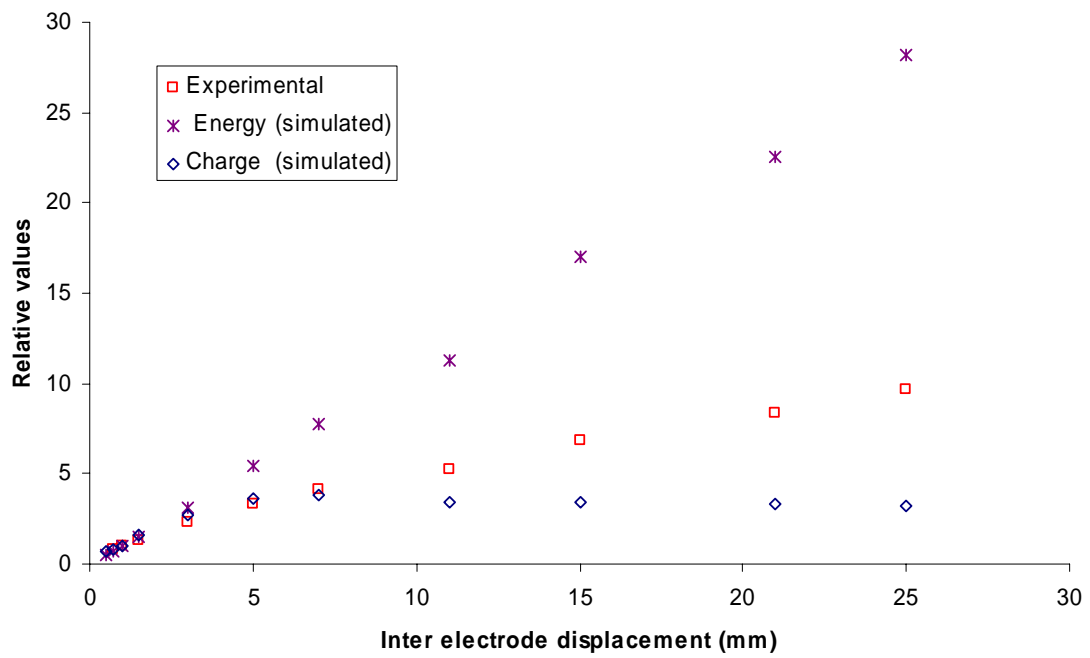


Figure 7

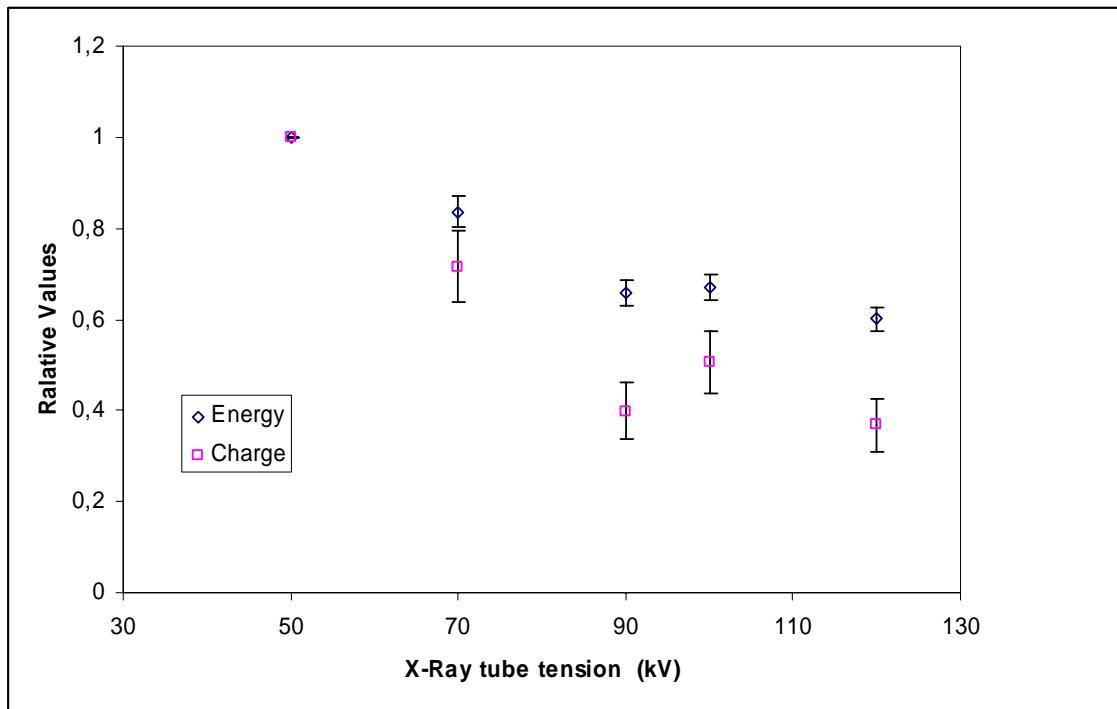


Figure 8

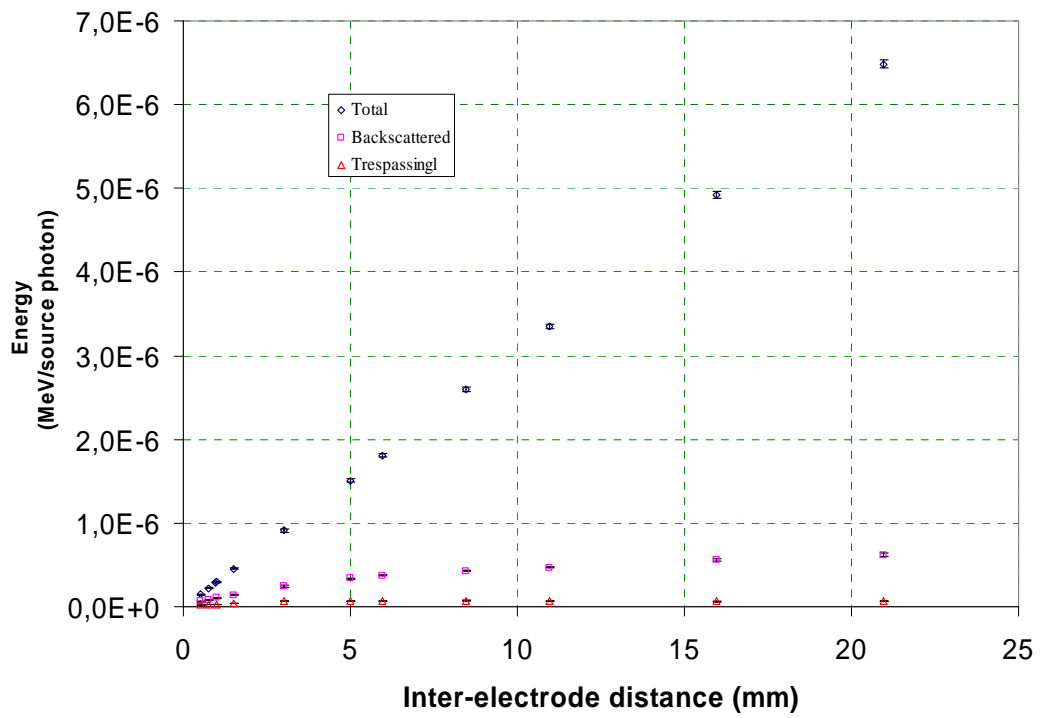


Figure 9

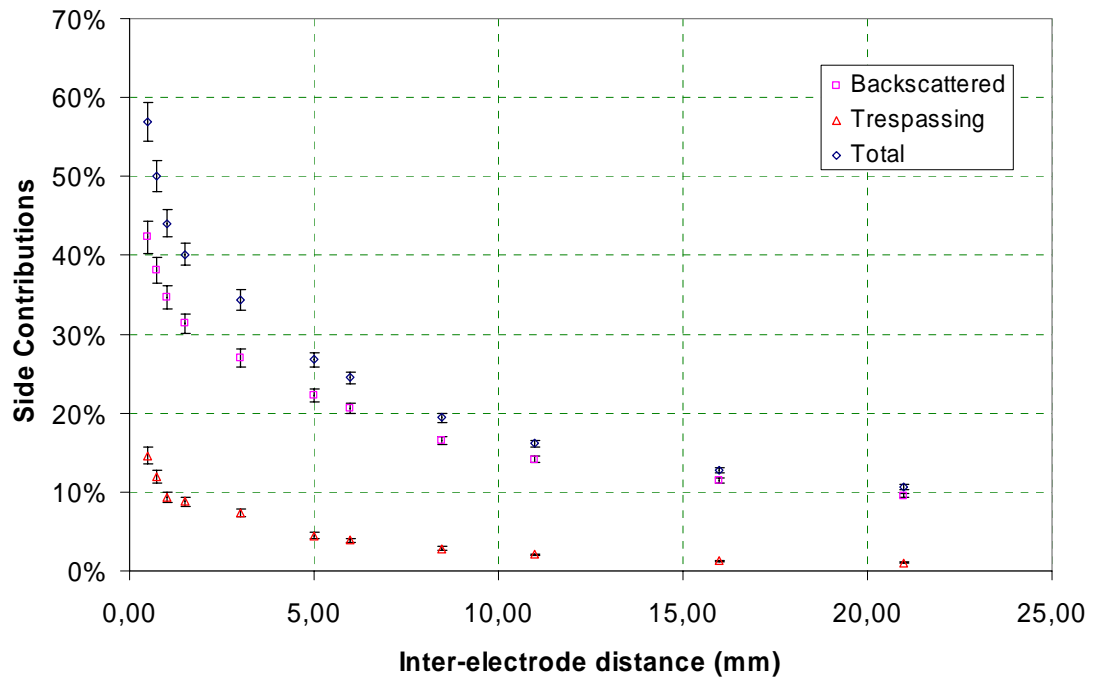


Figure 10